Adaptive Inverse Dynamics 4-Channel Control of Uncertain Nonlinear Teleoperation Systems

Xia Liu [1, 2] and Mahdi Tavakoli [2]

[1] School of Automation Engineering, University of Electronic Science and Technology of China, Chengdu, Sichuan, China 610054

[2] Department of Electrical and Computer Engineering, University of Alberta, Edmonton, Alberta, Canada T6G 2V4

Email: xia8@ualberta.ca, tavakoli@ece.ualberta.ca

Abstract

Most of the methods to date on bilateral control of nonlinear teleoperation systems lead to nonlinear and coupled closed-loop dynamics even in the ideal case of perfect knowledge of the master, the slave, the human operator and the environment. Consequently, the transparency of these closed-loop systems is difficult to study. In comparison, inverse dynamics controllers can deal with the nonlinear terms in the dynamics in a way that, in the ideal case, the closed-loop systems become linear and decoupled. In this paper, for multi-DOF nonlinear teleoperation systems with uncertainties, adaptive inverse dynamics controllers are incorporated into the 4-channel bilateral teleoperation control framework. The resulting controllers do not need exact knowledge of the dynamics of the master, the slave, the human operator, or the environment. A Lyapunov analysis is presented to prove the transparency of the teleoperation system. Simulations are also presented to show the effectiveness of the proposed approach.

Keywords: Bilateral teleoperation, transparency, uncertainties, adaptive inverse dynamics control

1. INTRODUCTION

Teleoperation systems have been widely applied to the environments that are too remote, too confined, or too hazardous for the human to be in. Outer space and undersea exploration, minimally invasive telesurgery, nuclear waste site and radioactive material management are typical examples. A teleoperation system consists of a user-interface robot (master), a teleoperated robot (slave), a human operator, and an environment – a general block diagram is depicted in Fig. 1. The human operator applies force (f_h) on the master to control the position of the slave (x_s) in order to perform a task in the remote environment. When the slave-environment contact force is reflected to the operator, the teleoperation is said to be bilateral. If the slave exactly reproduces the master's position trajectory (x_m) for the environment and the master accurately displays slave-environment contact force (f_e) to the human operator, the

teleoperation system is said to be fully transparent. For a review of teleoperation control approaches, see the survey papers [1], [2], [3].

Fig. 1 Block diagram of a general teleoperation system

A number of control schemes have been proposed for teleoperation systems with linear master and slave robots [4], [5], among which the 4-channel control architecture is the most successful in terms of ensuring full transparency [6], [7]. These fixed controllers assume perfect knowledge of the master and the slave impedances. In a teleoperation system, however, the perfect knowledge of the master and the slave dynamic models may not be available due to model uncertainties. Evidently, the control of teleoperation systems subject to model uncertainties poses significantly more challenges compared to the control of those with fixed models/parameters. In the following, we review the pertinent research results about adaptive control of teleoperation systems (roughly, in the order of increasing complexity).

There are a few adaptive control schemes in the literature for linear master and slave models where the slave and the environment dynamics are allowed to be uncertain. Lee and Chung [8] designed an adaptive control scheme for teleoperation systems with parametric uncertainties in the slave and the environment dynamics. Shi et al. [9] developed adaptive control schemes for teleoperation systems with different types of parametric uncertainties in the slave and the environments. In both of these, (a) the dynamics of the master and the slave were assumed to be 1-DOF and linear, and (b) an adaptive controller was designed for the slave, but a compensator was used for the master.

Adaptive control for nonlinear master and slave models is more challenging compared to those for linear ones. For this case, Ryu and Kwon [10] achieved position and force tracking when the environment's and the human operator's uncertain parameters were not included in the adaption. Hung et al. [11] designed adaptive bilateral controllers for both the nonlinear master and the nonlinear slave by introducing a virtual master to achieve position and force tracking performance. Chopra et al. [12] proposed an adaptive controller for a nonlinear teleoperator with time delay to ensure synchronization of positions and velocities of the master and the slave. Nuño et al. [13] showed that Chopra's scheme was applicable only to systems without gravity, and proposed a new adaptive controller to remove this constraint.

The limitation of the above methods is that they only consider the dynamic uncertainties of the master and the slave, and ignore the uncertainties introduced by the human operator and the environment. For nonlinear master and slave dynamics and linear human and environment dynamical models, all subject to parametric uncertainties, Zhu and Salcudean [14], Sirouspour and Setoodeh [15], and Malysz and Sirouspour [16] designed separate adaptive laws for the master and for the slave.

Nevertheless, this and other adaptive schemes are based on standard Slotine & Li adaptive control [17] and none of them has taken advantage of the inverse dynamics approach, which has the advantage of providing a nonlinear feedback control law that would cancel the nonlinear terms in the closed-loop dynamics if the dynamics were perfectly known. Adaptive inverse dynamics control of the position of a single robot under dynamic uncertainties was

investigated in [18], [19], [20]. Nonetheless, the results in [18], [19], [20] have only been applied to motion control of a single robot in free motion. So far, there has been no attempt at simultaneous motion and force control in a master-slave teleoperation system, in which the master and the slave are allowed to make contact with the human operator and the environment, respectively.

This paper proposes adaptive bilateral controllers based on the inverse dynamics approach for teleoperation systems with uncertain dynamics in the master, the slave, the operator, and the environment. The adaptive inverse dynamics controllers are incorporated into the 4-channel bilateral teleoperation control framework. In order to demonstrate the advantages of the proposed adaptive control scheme, it has been compared to the previous adaptive schemes for teleoperation systems from different aspects in Table 1. As Table 1 shows, the proposed control scheme is appropriate for master and slave robots with nonlinear n-DOF dynamics, and involves adaptive control of both the master and the slave (i.e., dynamic uncertainties in both the master and the slave are allowed). Besides, the proposed control scheme can also work where the dynamics of the operator and the environment are uncertain.

Table 1: A comparison of different adaptive control approaches for bilateral teleoperation systems

	[8]-[9]	[10]-[13]	[14]-[16]	This paper
Master dynamics	Linear, certain	Nonlinear, uncertain	Nonlinear, uncertain	Nonlinear, uncertain
Slave dynamics	Linear, uncertain	Nonlinear, uncertain	Nonlinear, uncertain	Nonlinear, uncertain
Master controller	Fixed	Adaptive	Adaptive	Adaptive
Slave controller	Adaptive	Adaptive	Adaptive	Adaptive
Operator	Certain	Certain	Uncertain	Uncertain
Environment	Uncertain	Certain	Uncertain	Uncertain
DOF	1-DOF	n-DOF	n-DOF	n-DOF
Scheme	Slotine&Li based	Slotine&Li based	Slotine&Li based	inverse dynamics

The rest of this paper is organized as follows. In Section 2, various teleoperation control architectures are compared with respect to their transparency. In Section 3, nonlinear model of teleoperation systems is given. In Section 4, the 4-channel control architecture is modified to encompass adaptive inverse dynamics controllers for the master and the slave. A Lyapunov function is constructed for the unified closed-loop, and transparency of the overall system is investigated. In Section 5, an alternate control scheme is discussed that explicitly addresses the uncertain dynamics of the human operator and the environment. In Section 6, simulations are done to show the effectiveness of the proposed controller. The paper is concluded in Section 7.

2. VARIOUS TELEOPERATION CONTROL ARCHITECTURES

For precise teleoperation, transparency is essential. In an ideally transparent teleoperation system, through appropriate control signals, the master and the slave positions and forces will match regardless of the operator and environment dynamics, i.e.,

$$x_m = x_s, \ f_h = f_e \tag{1}$$

To evaluate the transparency of teleoperation, the hybrid matrix is used which is defined as

$$\begin{bmatrix} f_h \\ -x_s \end{bmatrix} = \begin{bmatrix} h_{11} & h_{12} \\ h_{21} & h_{22} \end{bmatrix} \begin{bmatrix} x_m \\ f_e \end{bmatrix} \tag{2}$$

Thus, full transparency is achieved if and only if the hybrid matrix has the following form:

$$H_{ideal} = \begin{bmatrix} 0 & 1 \\ -1 & 0 \end{bmatrix} \tag{3}$$

The hybrid parameter $h_{11} = f_h/x_m(f_e = 0)$ is the input impedance in the free-motion condition. Nonzero values for h_{11} mean that even when the slave is in free space, the user will receive some force feedback, thus giving a "sticky" feel of free-motion movements. The parameter $h_{12} = f_h/f_e(x_m = 0)$ is a measure of force tracking for the haptic teleoperation system when the master is locked in motion (perfect force tracking for $h_{12} = 1$). The parameter $h_{21} = -x_s/x_m(f_e = 0)$ is a measure of position (velocity) tracking performance when the slave is in free space (perfect position or velocity tracking for $h_{21} = -1$). The parameter $h_{22} = -x_s/f_e(x_m = 0)$ is the output admittance when the master is locked in motion. Nonzero values for h_{22} indicate that even when the master is locked in place, the slave will move in response to slave/environment contacts.

For achieving the ideal response, various teleoperation control architectures are proposed [21], [22], [23], [24]: Position Error Based (PEB), Direct Force Reflection (DFR), Shared Compliance Control (SCC), and 4-channel Control. In the following, we compare the transparency of these control architectures.

2.1 PEB

A position-error-based, also called position–position, teleoperation architecture is shown in Fig. 2(a). The impedances $Z_m(s)$ and $Z_s(s)$ represent the dynamic characteristics of the master robot and the slave robot, respectively. Also, C_L and C_R are proportional-derivative controllers that are used at the master and the slave, respectively.

As can be seen in Fig. 2(a) – the signals f_h^* and f_e^* denote the exogenous forces of the operator and the environment, respectively – the PEB controller does not use any force sensor measurements and merely tries to minimize the difference between the master and the slave positions, thus reflecting a force proportional to this difference to the user once the slave makes contact with an object. The hybrid matrix for this architecture can be found as

$$H = \begin{bmatrix} Z_m + C_L \frac{Z_s}{Z_{ts}} & \frac{C_L}{Z_{ts}} \\ -\frac{C_R}{Z_{ts}} & \frac{1}{Z_{ts}} \end{bmatrix} \tag{4}$$

where $Z_{tm} = Z_m + C_L$ and $Z_{ts} = Z_s + C_R$. As a result, in addition to non-ideal force tracking ($h_{12} \neq 1$), the PEB method suffers from a distorted perception in free-motion condition ($h_{11} \neq 0$). This means that in the absence of a slave-side force sensor, control inaccuracies (i.e., nonzero position errors) lead to force feedback to the user even when the slave is not in contact with the environment.

2.2 DFR

A direct force reflection, also called force–position, teleoperation architecture is shown in Fig. 2(b). This method requires a force sensor to measure the interaction between the slave and the environment. The hybrid parameters for the DFR architecture are given as

$$H = \begin{bmatrix} Z_m & 1 \\ -\frac{C_R}{Z_{ts}} & \frac{1}{Z_{ts}} \end{bmatrix} \tag{5}$$

Although the perception of free motion is still less than ideal ($h_{11} \neq 0$), a perfect force tracking performance is attained ($h_{12} = 1$). Nonetheless, compared to the PEB method, h_{11} is much closer to zero in the DFR method, and the user only feels the inertia of the master interface when the slave is in free motion. Although the DFR method's transparency is somewhat better than the PEB method, both methods suffer from the less-than-ideal h_{21} and h_{22} values.

2.3 SCC

A shared compliance control, also called impedance control, teleoperation architecture is shown in Fig. 2(c). In this method, for the master, the control is the same as in DFR. But for the slave, the control includes position control terms as well as the measured interaction force between the slave and the environment. The hybrid parameters for this architecture are given as

$$H = \begin{bmatrix} Z_m & 1 \\ -\frac{C_R}{Z_{ts}} & \frac{1+C_5}{Z_{ts}} \end{bmatrix} \tag{6}$$

As we can see from the hybrid matrix H, impedance control methods still suffers from the less-than-ideal h_{21} and h_{22} values.

2.4 4-channel Control

Fig. 2(d) depicts a 4-channel bilateral teleoperation architecture. This architecture can represent the previous teleoperation structures through appropriate selection of controllers C_1 to C_6. The compensators C_5 and C_6 in Fig. 2(d) constitute a local force feedback at the slave side and the master side, respectively. The hybrid parameters for the 4-channel architecture are

$$h_{11} = (Z_{ts}Z_{tm} + C_1C_4)/D$$
$$h_{12} = [Z_{ts}C_2 - (1 + C_5)C_4]/D$$
$$h_{21} = -[Z_{tm}C_3 + (1 + C_6)C_1]/D \tag{7}$$
$$h_{22} = -[C_2C_3 - (1 + C_5)(1 + C_6)]/D$$

where $D = -C_3C_4 + Z_{ts}(1 + C_6)$.

In contrast to the PEB, DFR, and SCC architectures, a sufficient number of parameters in the 4-channel architecture enable it to achieve ideal transparency. In fact, by selecting C_1 through C_6 according to

$$C_1 = Z_{ts} \quad C_2 = 1 + C_6 \quad C_3 = 1 + C_5 \quad C_4 = -Z_{tm} \tag{8}$$

the ideal transparency conditions is achieved, i.e.,

$$H = \begin{bmatrix} 0 & 1 \\ -1 & 0 \end{bmatrix} \tag{9}$$
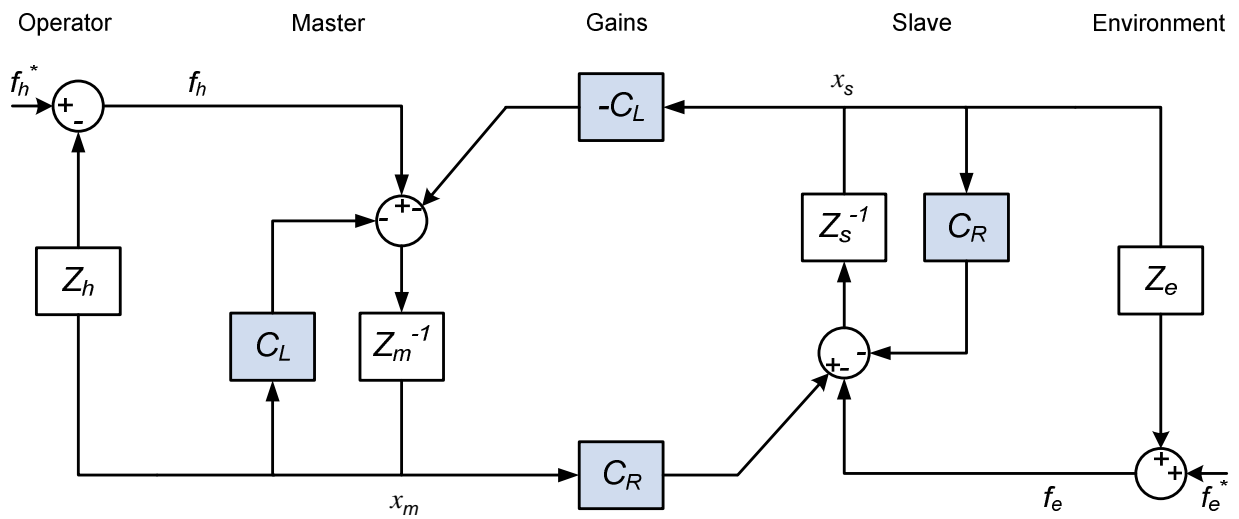
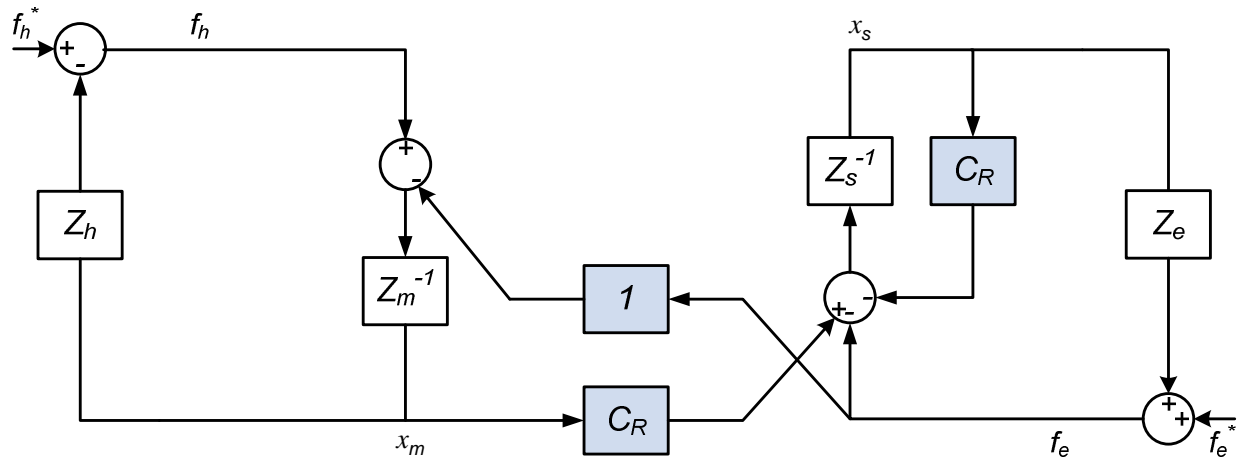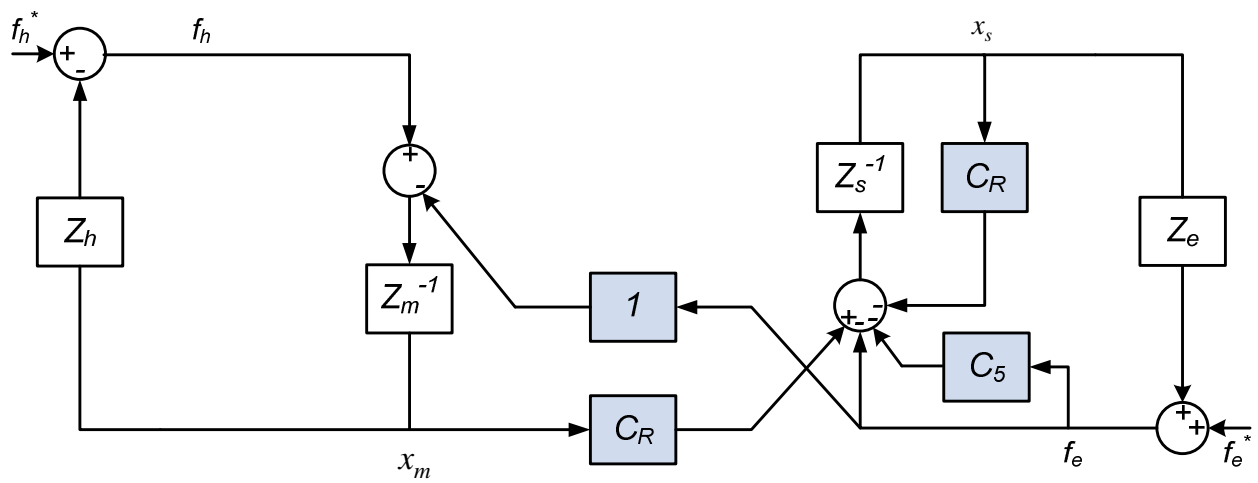Fig. 2(a) PEB architecture

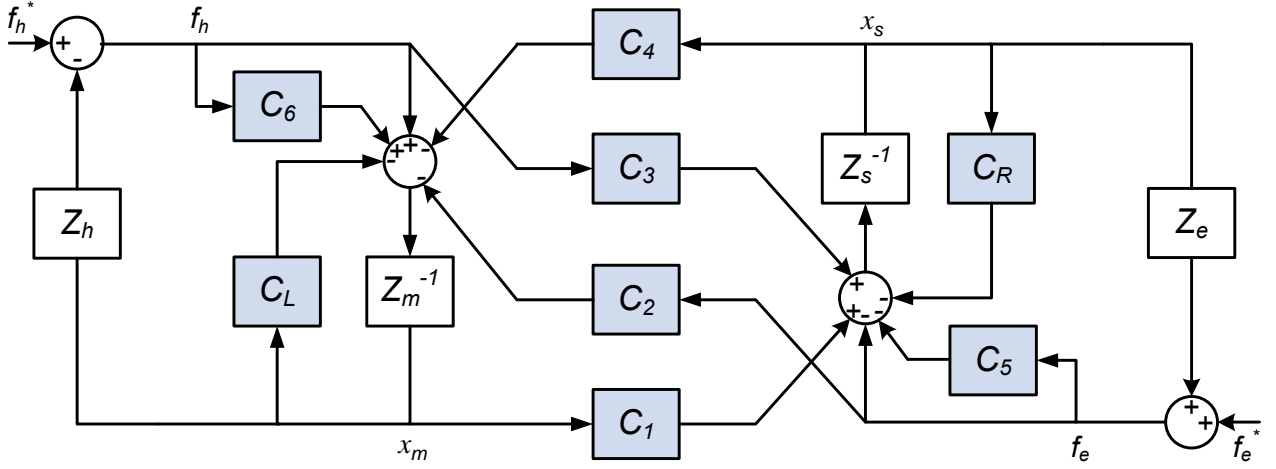

Fig. 2(b) DFR architecture

Fig. 2(c) SCC architecture

Fig. 2(d) 4-channel architecture

3. NONLINEAR MODELS OF TELEOPERATION SYSTEMS

In practice, it is desirable to express the dynamics of the master and the slave robots (and ensure position and force tracking) in the Cartesian space, where the tasks and interactions with the operator and the environment are naturally specified. In this section, we develop the nonlinear model of teleoperation system in Cartesian Space.

3.1 Robot Dynamics Transformation from Joint Space to Cartesian Space

The general dynamics of a n-DOF robot in the joint space is as follows [25], [26]:

$$\mathbf{M}(\mathbf{q})\ddot{\mathbf{q}} + \mathbf{C}(\mathbf{q}, \dot{\mathbf{q}})\dot{\mathbf{q}} + \mathbf{G}(\mathbf{q}) = \boldsymbol{\tau} \tag{10}$$

where $\mathbf{q} \in \mathrm{R}^{n\times 1}$ is the joint angle, $\mathbf{M}(\mathbf{q}) \in \mathrm{R}^{n\times n}$ is the inertia matrix, $\mathbf{C}(\mathbf{q}, \dot{\mathbf{q}}) \in \mathrm{R}^{n\times n}$ is the Coriolis and centrifugal term, $\mathbf{G}(\mathbf{q}) \in \mathrm{R}^{n\times 1}$ is the gravity term, and $\boldsymbol{\tau} \in \mathrm{R}^{n\times 1}$ is the exerted joint torque. Note that the forces acting on the end-effector, $\mathbf{f}$, result in joint toques

$$\boldsymbol{\tau} = \mathbf{J}^{\mathrm{T}}(\mathbf{q})\mathbf{f} \tag{11}$$

where $\mathbf{J}$ is the Jacobian matrix. Multiplying both sides of (10) by $\mathbf{J}^{-\mathrm{T}}$, we get

$$\mathbf{J}^{-\mathrm{T}}\mathbf{M}(\mathbf{q})\ddot{\mathbf{q}} + \mathbf{J}^{-\mathrm{T}}\mathbf{C}(\mathbf{q}, \dot{\mathbf{q}})\dot{\mathbf{q}} + \mathbf{J}^{-\mathrm{T}}\mathbf{G}(\mathbf{q}) = \mathbf{J}^{-\mathrm{T}}\boldsymbol{\tau} = \mathbf{f} \tag{12}$$

On the other hand, we have the relationship

$$\dot{\mathbf{x}} = \mathbf{J}\dot{\mathbf{q}} \tag{13}$$

where $\dot{\mathbf{x}}$ is Cartesian-space velocity. Differentiating (13), we obtain

$$\ddot{\mathbf{x}} = \dot{\mathbf{J}}\dot{\mathbf{q}} + \mathbf{J}\ddot{\mathbf{q}} \tag{14}$$

Thus,

$$\dot{\mathbf{q}} = \mathbf{J}^{-1}\dot{\mathbf{x}} \tag{15}$$

$$\ddot{\mathbf{q}} = \mathbf{J}^{-1}\ddot{\mathbf{x}} - \mathbf{J}^{-1}\dot{\mathbf{J}}\mathbf{J}^{-1}\dot{\mathbf{x}} \tag{16}$$

Substituting (15) and (16) into (12), we can derive the equivalent of the dynamics (10) in the Cartesian space as

$$\mathbf{M}_{\mathrm{x}}(\mathbf{q})\ddot{\mathbf{x}} + \mathbf{C}_{\mathrm{x}}(\mathbf{q}, \dot{\mathbf{q}})\dot{\mathbf{x}} + \mathbf{G}_{\mathrm{x}}(\mathbf{q}) = \mathbf{f} \tag{17}$$

where

$$\mathbf{M}_x(\mathbf{q}) = \mathbf{J}^{-T}\mathbf{M}(\mathbf{q})\mathbf{J}^{-1}, \mathbf{C}_x(\mathbf{q},\dot{\mathbf{q}}) = \mathbf{J}^{-T}\mathbf{C}(\mathbf{q},\dot{\mathbf{q}})\mathbf{J}^{-1} - \mathbf{M}_x(\mathbf{q})\dot{\mathbf{J}}\mathbf{J}^{-1}, \mathbf{G}_x(\mathbf{q}) = \mathbf{J}^{-T}\mathbf{G}(\mathbf{q})$$

3.2 Nonlinear Model of Teleoperation System in Cartesian Space

According to (17), when interacting with a human and an environment, the Cartesian-space nonlinear dynamic models for n-DOF master and slave robots can be written as,

$$\mathbf{M}_{xm}(\mathbf{q}_m)\ddot{\mathbf{x}}_m + \mathbf{C}_{xm}(\mathbf{q}_m,\dot{\mathbf{q}}_m)\dot{\mathbf{x}}_m + \mathbf{G}_{xm}(\mathbf{q}_m) = \mathbf{f}_m + \mathbf{f}_h \tag{18}$$

$$\mathbf{M}_{xs}(\mathbf{q}_s)\ddot{\mathbf{x}}_s + \mathbf{C}_{xs}(\mathbf{q}_s,\dot{\mathbf{q}}_s)\dot{\mathbf{x}}_s + \mathbf{G}_{xs}(\mathbf{q}_s) = \mathbf{f}_s - \mathbf{f}_e \tag{19}$$

where $\mathbf{x}_m, \mathbf{x}_s \in R^{6\times1}$ are end-effector Cartesian positions (and orientations), $\mathbf{q}_m, \mathbf{q}_s \in R^{n\times1}$ are joint angle positions, $\mathbf{M}_{xm}(\mathbf{q}_m), \mathbf{M}_{xs}(\mathbf{q}_s) \in R^{6\times6}$ are symmetric positive-definite inertia matrices, $\mathbf{C}_{xm}(\mathbf{q}_m,\dot{\mathbf{q}}_m), \mathbf{C}_{xs}(\mathbf{q}_s,\dot{\mathbf{q}}_s) \in R^{6\times6}$ are the Coriolis and centrifugal terms, and $\mathbf{G}_{xm}(\mathbf{q}_m), \mathbf{G}_{xs}(\mathbf{q}_s) \in R^{6\times1}$ are the gravity terms for the master and the slave, respectively. Also, $\mathbf{f}_m, \mathbf{f}_s \in R^{6\times1}$ are force/torque control signals (i.e., controller outputs) for the master and the slave, $\mathbf{f}_h \in R^{6\times1}$ is the force/torque that the operator applies to the master, and $\mathbf{f}_e \in R^{6\times1}$ is the force/ torque that the environment applies to the slave.

Property 1. The left sides of (18) and (19) are linear in a set of dynamic parameters $\boldsymbol{\theta}_{md} = (\theta_{md1}, \dots, \theta_{mdp_1})^T$ and $\boldsymbol{\theta}_{sd} = (\theta_{sd1}, \dots, \theta_{sdp_2})^T$ as [25], [26]

$$\mathbf{M}_{xm}(\mathbf{q}_m)\ddot{\mathbf{x}}_m + \mathbf{C}_{xm}(\mathbf{q}_m,\dot{\mathbf{q}}_m)\dot{\mathbf{x}}_m + \mathbf{G}_{xm}(\mathbf{q}_m) = \mathbf{Y}_{md}(\mathbf{q}_m,\dot{\mathbf{q}}_m,\dot{\mathbf{x}}_m,\ddot{\mathbf{x}}_m)\boldsymbol{\theta}_{md} \tag{20}$$

$$\mathbf{M}_{xs}(\mathbf{q}_s)\ddot{\mathbf{x}}_s + \mathbf{C}_{xs}(\mathbf{q}_s,\dot{\mathbf{q}}_s)\dot{\mathbf{x}}_s + \mathbf{G}_{xs}(\mathbf{q}_s) = \mathbf{Y}_{sd}(\mathbf{q}_s,\dot{\mathbf{q}}_s,\dot{\mathbf{x}}_s,\ddot{\mathbf{x}}_s)\boldsymbol{\theta}_{sd} \tag{21}$$

where $\mathbf{Y}_{md} \in R^{n\times p_1}$ and $\mathbf{Y}_{sd} \in R^{n\times p_2}$ are the dynamic regressor matrices for the master and the slave, respectively.

When the master and the slave experience parametric uncertainties, (20) and (21) become

$$\widehat{\mathbf{M}}_{xm}(\mathbf{q}_m)\ddot{\mathbf{x}}_m + \widehat{\mathbf{C}}_{xm}(\mathbf{q}_m,\dot{\mathbf{q}}_m)\dot{\mathbf{x}}_m + \widehat{\mathbf{G}}_{xm}(\mathbf{q}_m) = \mathbf{Y}_{md}\widehat{\boldsymbol{\theta}}_{md} \tag{22}$$

$$\widehat{\mathbf{M}}_{xs}(\mathbf{q}_s)\ddot{\mathbf{x}}_s + \widehat{\mathbf{C}}_{xs}(\mathbf{q}_s,\dot{\mathbf{q}}_s)\dot{\mathbf{x}}_s + \widehat{\mathbf{G}}_{xs}(\mathbf{q}_s) = \mathbf{Y}_{sd}\widehat{\boldsymbol{\theta}}_{sd} \tag{23}$$

where $\widehat{\boldsymbol{\theta}}_{md}$ and $\widehat{\boldsymbol{\theta}}_{sd}$ are the estimates of $\boldsymbol{\theta}_{md}$ and $\boldsymbol{\theta}_{sd}$, respectively.

4. ADAPTIVE INVERSE DYNAMICS 4-CHANNEL TELEOPERATION CONTROL

The basic idea of regular (i.e., non-adaptive) inverse dynamics control is to seek a nonlinear feedback law to cancel the nonlinear terms in a dynamic model. Our proposed teleoperation control scheme is based on incorporating two adaptive inverse dynamics controllers for the master and the slave (with dynamic uncertainties) into the 4-channel teleoperation architecture, as shown next.

4.1 Architecture of the Designed Control Approach

As it can be seen in the block diagram of the proposed architecture in Fig. 3, the position controller comprising C_L and C_4 for the master and C_R and C_1 for the slave are replaced by two designed adaptive inverse dynamics position controllers (the dashed boxes). The remaining terms C_2, C_3, C_5 and C_6 are still utilized as force feedback and feedforward controllers in the proposed approach. The block diagrams of the designed inverse dynamics position controllers for the master and the slave are shown in Fig. 4.
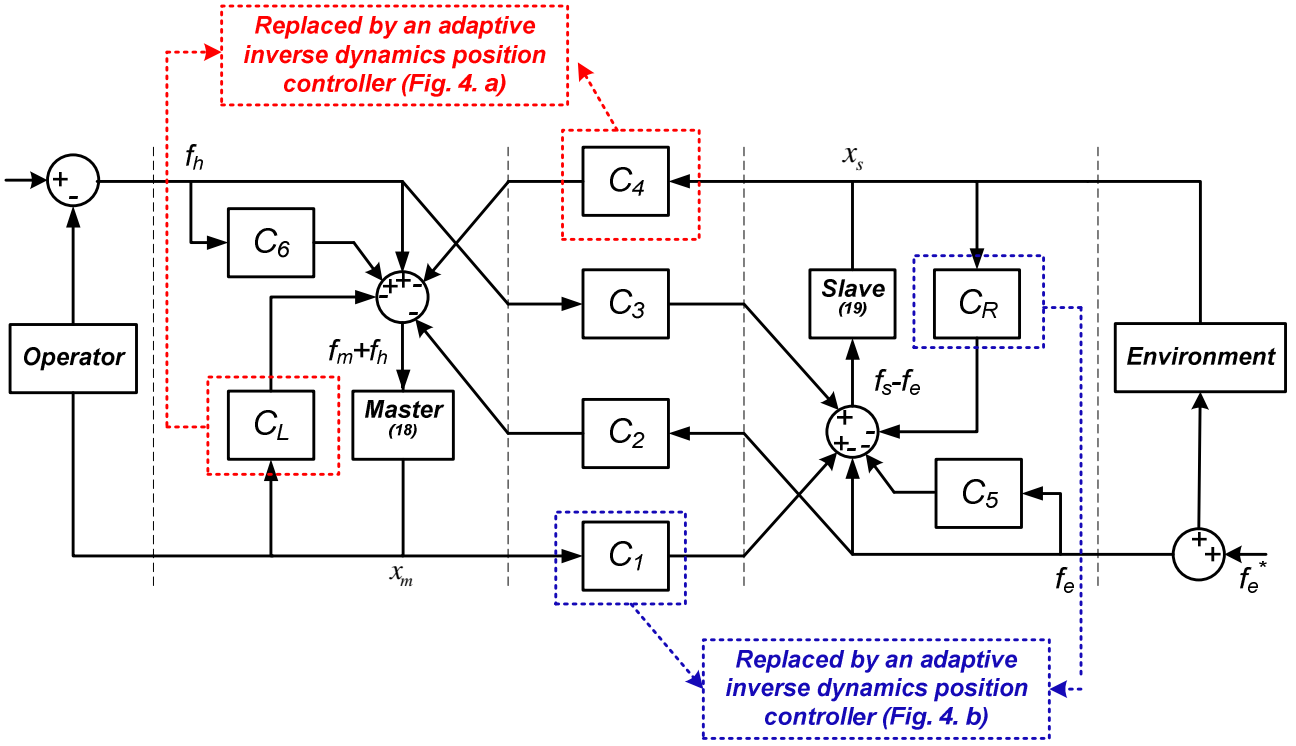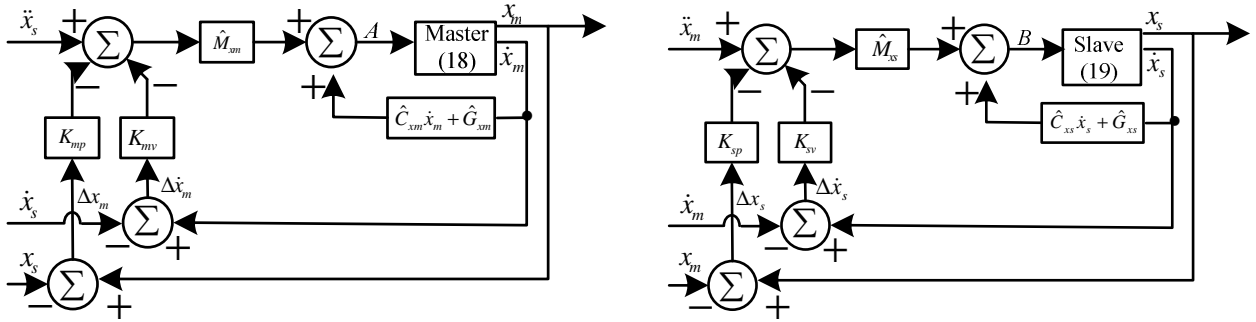
Fig. 3 4-channel adaptive inverse dynamics teleoperation control

$$\mathbf{A} = \widehat{\mathbf{M}}_{xm}\big(\ddot{\mathbf{x}}_s - K_{mv}\Delta\dot{\mathbf{x}}_m - K_{mp}\Delta\mathbf{x}_m\big) + \widehat{\mathbf{C}}_{xm}\dot{\mathbf{x}}_m + \widehat{\mathbf{G}}_{xm} \qquad \mathbf{B} = \widehat{\mathbf{M}}_{xs}\big(\ddot{\mathbf{x}}_m - K_{sv}\Delta\dot{\mathbf{x}}_s - K_{sp}\Delta\mathbf{x}_s\big) + \widehat{\mathbf{C}}_{xs}\dot{\mathbf{x}}_s + \widehat{\mathbf{G}}_{xs}$$

Fig. 4 Adaptive inverse dynamics position controllers (a) for the master (left) and (b) for the slave (right)

4.2 Control Laws and Adaptation Laws

We are now in a position to propose our adaptive inverse dynamics bilateral control algorithm for the uncertain nonlinear teleoperation systems. The controllers are designed for both the master and the slave.

- Control laws for the master and the slave:

$$\mathbf{f}_m = \widehat{\mathbf{M}}_{xm}(\mathbf{q}_m)\big(\ddot{\mathbf{x}}_s - K_{mv}\Delta\dot{\mathbf{x}}_m - K_{mp}\Delta\mathbf{x}_m\big) + \widehat{\mathbf{C}}_{xm}(\mathbf{q}_m, \dot{\mathbf{q}}_m)\dot{\mathbf{x}}_m + \widehat{\mathbf{G}}_{xm}(\mathbf{q}_m) + \widehat{\mathbf{M}}_{xm}(\mathbf{q}_m)C_2(\mathbf{f}_h - \mathbf{f}_e) - \mathbf{f}_h \qquad (24)$$

$$\mathbf{f}_s = \widehat{\mathbf{M}}_{xs}(\mathbf{q}_s)\big(\ddot{\mathbf{x}}_m - K_{sv}\Delta\dot{\mathbf{x}}_s - K_{sp}\Delta\mathbf{x}_s\big) + \widehat{\mathbf{C}}_{xs}(\mathbf{q}_s, \dot{\mathbf{q}}_s)\dot{\mathbf{x}}_s + \widehat{\mathbf{G}}_{xs}(\mathbf{q}_s) + \widehat{\mathbf{M}}_{xs}(\mathbf{q}_s)C_3(\mathbf{f}_h - \mathbf{f}_e) + \mathbf{f}_e \qquad (25)$$

where $\Delta\mathbf{x}_m = \mathbf{x}_m - \mathbf{x}_s$, $\Delta\mathbf{x}_s = \mathbf{x}_s - \mathbf{x}_m$, and $K_{mv}, K_{sv}, K_{mp}, K_{sp}, C_2$ and C_3 can all be chosen to be positive constants.

- Adaptation laws for the master and the slave:

$$\hat{\dot{\boldsymbol{\theta}}}_{md} = -\mathbf{L}_{md}[\boldsymbol{\Phi}_m^T(\Delta\dot{\mathbf{x}}_m + \alpha\Delta\mathbf{x}_m) + \mathbf{W}_m^T\mathbf{E}_m] \tag{26}$$

$$\hat{\dot{\boldsymbol{\theta}}}_{sd} = -\mathbf{L}_{sd}[\boldsymbol{\Phi}_s^T(\Delta\dot{\mathbf{x}}_s + \alpha\Delta\mathbf{x}_s) + \mathbf{W}_s^T\mathbf{E}_s] \tag{27}$$

where $\mathbf{L}_{md}$ and $\mathbf{L}_{sd}$ are symmetric positive-definite matrices, α is a positive constant and is chosen such that $\alpha < K_v$ (K_v will be defined later in this section). Also,

$$\boldsymbol{\Phi}_m = (1/(1 + C_2/C_3))\hat{\mathbf{M}}_{xm}^{-1}(\mathbf{q}_m)\mathbf{Y}_{md} \tag{28}$$

$$\boldsymbol{\Phi}_s = (1/(1 + C_2/C_3))(C_2/C_3)\hat{\mathbf{M}}_{xs}^{-1}(\mathbf{q}_s)\mathbf{Y}_{sd} \tag{29}$$

Besides, $\mathbf{E}_m$ and $\mathbf{E}_s$ are filtered prediction errors of the form

$$\mathbf{E}_m = \mathbf{W}_m\hat{\boldsymbol{\theta}}_{md} - \mathbf{f}_{mw} - \mathbf{f}_{hw} \tag{30}$$

$$\mathbf{E}_s = \mathbf{W}_s\hat{\boldsymbol{\theta}}_{sd} - \mathbf{f}_{sw} + \mathbf{f}_{ew} \tag{31}$$

where $\mathbf{f}_{mw}$, $\mathbf{f}_{hw}$, $\mathbf{f}_{sw}$ and $\mathbf{f}_{ew}$ are the filtered versions of the forces $\mathbf{f}_m$, $\mathbf{f}_h$, $\mathbf{f}_s$ and $\mathbf{f}_e$, respectively. The subscript w shows low-pass filtering by the filter $\frac{\lambda}{s+\lambda}$, e.g. $\mathbf{f}_{mw} = \frac{\lambda}{s+\lambda}\mathbf{f}_m$, where λ is a positive constant and s is the Laplace operator. Also, $\mathbf{W}_m$ and $\mathbf{W}_s$ are filtered versions of the dynamic regressor matrices $\mathbf{Y}_{md}$ and $\mathbf{Y}_{sd}$.

Each of the control laws (24)-(25) includes five parts. In the master controller (24), the first part $\hat{\mathbf{M}}_{xm}(\mathbf{q}_m)(\ddot{\mathbf{x}}_s - K_{mv}\Delta\dot{\mathbf{x}}_m - K_{mp}\Delta\mathbf{x}_m)$, the second part $\hat{\mathbf{C}}_{xm}(\mathbf{q}_m, \dot{\mathbf{q}}_m)\dot{\mathbf{x}}_m$ and the third part $\hat{\mathbf{G}}_{xm}(\mathbf{q}_m)$ altogether perform the adaptive inverse dynamics position control (see Fig. 4(a)). The fourth part $\hat{\mathbf{M}}_{xm}(\mathbf{q}_m)C_2(\mathbf{f}_h - \mathbf{f}_e)$ involves force feedback. The fifth part $-\mathbf{f}_h$ compensates for the force due to the operator. The five parts in the slave controller (25) have similar meanings.

Substituting (24)-(25) into (18)-(19), the closed-loop equations of the master and the slave are obtained as

$$\mathbf{M}_{xm}(\mathbf{q}_m)\ddot{\mathbf{x}}_m + \mathbf{C}_{xm}(\mathbf{q}_m, \dot{\mathbf{q}}_m)\dot{\mathbf{x}}_m + \mathbf{G}_{xm}(\mathbf{q}_m) =$$
$$\hat{\mathbf{M}}_{xm}(\mathbf{q}_m)(\ddot{\mathbf{x}}_s - K_{mv}\Delta\dot{\mathbf{x}}_m - K_{mp}\Delta\mathbf{x}_m) + \hat{\mathbf{C}}_{xm}(\mathbf{q}_m, \dot{\mathbf{q}}_m)\dot{\mathbf{x}}_m + \hat{\mathbf{G}}_{xm}(\mathbf{q}_m) + \hat{\mathbf{M}}_{xm}(\mathbf{q}_m)C_2(\mathbf{f}_h - \mathbf{f}_e) \tag{32}$$

$$\mathbf{M}_{xs}(\mathbf{q}_s)\ddot{\mathbf{x}}_s + \mathbf{C}_{xs}(\mathbf{q}_s, \dot{\mathbf{q}}_s)\dot{\mathbf{x}}_s + \mathbf{G}_{xs}(\mathbf{q}_s) =$$
$$\hat{\mathbf{M}}_{xs}(\mathbf{q}_s)(\ddot{\mathbf{x}}_m - K_{sv}\Delta\dot{\mathbf{x}}_s - K_{sp}\Delta\mathbf{x}_s) + \hat{\mathbf{C}}_{xs}(\mathbf{q}_s, \dot{\mathbf{q}}_s)\dot{\mathbf{x}}_s + \hat{\mathbf{G}}_{xs}(\mathbf{q}_s) + \hat{\mathbf{M}}_{xs}(\mathbf{q}_s)C_3(\mathbf{f}_h - \mathbf{f}_e) \tag{33}$$

Adding $\hat{\mathbf{M}}_{xm}(\mathbf{q}_m)\ddot{\mathbf{x}}_m$ and then subtracting it in the right side of (32) helps to rewrite it as

$$\hat{\mathbf{M}}_{xm}(\mathbf{q}_m)(\Delta\ddot{\mathbf{x}}_m + K_{mv}\Delta\dot{\mathbf{x}}_m + K_{mp}\Delta\mathbf{x}_m) = \mathbf{Y}_{md}\Delta\boldsymbol{\theta}_{md} + \hat{\mathbf{M}}_{xm}(q_m)C_2(\mathbf{f}_h - \mathbf{f}_e) \tag{34}$$

Similarly, (33) can be rewritten as

$$\hat{\mathbf{M}}_{xs}(\mathbf{q}_s)(\Delta\ddot{\mathbf{x}}_s + K_{sv}\Delta\dot{\mathbf{x}}_s + K_{sp}\Delta\mathbf{x}_s) = \mathbf{Y}_{sd}\Delta\boldsymbol{\theta}_{sd} + \hat{\mathbf{M}}_{xs}(\mathbf{q}_s)C_3(\mathbf{f}_h - \mathbf{f}_e) \tag{35}$$

Multiplying both sides of (34) and (35) by $\hat{\mathbf{M}}_{xm}^{-1}(\mathbf{q}_m)$ and $\hat{\mathbf{M}}_{xs}^{-1}(\mathbf{q}_s)$, respectively, the closed-loop equations of the master and the slave can be rewritten as

$$\Delta\ddot{\mathbf{x}}_m + K_{mv}\Delta\dot{\mathbf{x}}_m + K_{mp}\Delta\mathbf{x}_m - \hat{\mathbf{M}}_{xm}^{-1}(\mathbf{q}_m)\mathbf{Y}_{md}\Delta\boldsymbol{\theta}_{md} = C_2(\mathbf{f}_h - \mathbf{f}_e) \tag{36}$$

$$\Delta\ddot{\mathbf{x}}_s + K_{sv}\Delta\dot{\mathbf{x}}_s + K_{sp}\Delta\mathbf{x}_s - \hat{\mathbf{M}}_{xs}^{-1}(\mathbf{q}_s)\mathbf{Y}_{sd}\Delta\boldsymbol{\theta}_{sd} = C_3(\mathbf{f}_h - \mathbf{f}_e) \tag{37}$$

where $\Delta\boldsymbol{\theta}_{md} = \hat{\boldsymbol{\theta}}_{md} - \boldsymbol{\theta}_{md}$ and $\Delta\boldsymbol{\theta}_{sd} = \hat{\boldsymbol{\theta}}_{sd} - \boldsymbol{\theta}_{sd}$.

Now, multiplying both sides of (37) by C_2/C_3, using the fact that $\Delta\mathbf{x}_m = -\Delta\mathbf{x}_s$, $\Delta\dot{\mathbf{x}}_m = -\Delta\dot{\mathbf{x}}_s$ and $\Delta\ddot{\mathbf{x}}_m = -\Delta\ddot{\mathbf{x}}_s$, and subtracting (36) from the result, we arrive at the following unified closed-loop dynamics for the master and the slave:

$$(1 + C_2/C_3)\Delta\ddot{\mathbf{x}}_m + (K_{mv} + (C_2/C_3)K_{sv})\Delta\dot{\mathbf{x}}_m + (K_{mp} + (C_2/C_3)K_{sp})\Delta\mathbf{x}_m - \hat{\mathbf{M}}_{xm}^{-1}(q_m)\mathbf{Y}_{md}\Delta\boldsymbol{\theta}_{md}$$

$$+(C_2/C_3)\widehat{\mathbf{M}}_{xs}^{-1}(q_s)\mathbf{Y}_{sd}\Delta\boldsymbol{\theta}_{sd} = 0 \tag{38}$$

Multiplying both sides of (38) by $1/(1 + C_2/C_3)$, the *unified closed-loop* can be rewritten as

$$\Delta\ddot{\mathbf{x}}_m + K_v\Delta\dot{\mathbf{x}}_m + K_p\Delta\mathbf{x}_m = \boldsymbol{\Phi}_m\Delta\boldsymbol{\theta}_{md} - \boldsymbol{\Phi}_s\Delta\boldsymbol{\theta}_{sd} \tag{39}$$

where

$$K_v = (1/(1 + C_2/C_3))(K_{mv} + (C_2/C_3)K_{sv}), K_p = (1/(1 + C_2/C_3))(K_{mp} + (C_2/C_3)K_{sp})$$

Since $K_{mv}, K_{sv}, K_{mp}, K_{sp}, C_2$ and C_3 are all positive constants, K_v and K_p are also positive constants. It should be noted that, the left side of the unified closed-loop system (39) is a linear error expression under the role the designed adaptive inverse dynamics controllers (24)-(25). Furthermore, once the parameters converge to their true values, i.e., $\Delta\boldsymbol{\theta}_{md} = \Delta\boldsymbol{\theta}_{sd} = 0$, the linear closed-loop system (39) will become completely decoupled as $\Delta\ddot{\mathbf{x}}_m + K_v\Delta\dot{\mathbf{x}}_m + K_p\Delta\mathbf{x}_m = 0$. Thus, the performance of the system is very convenient to study.

Remark 1: We obtained the unified closed-loop dynamics (39) for the overall teleoperation system based on the master closed-loop dynamics (36) and the slave closed-loop dynamics (37). Thus, we can use a unified Lyapunov function to show the transparency of the overall system as in the next section.

Remark 2: It is possible to generalize $K_{mv}, K_{sv}, K_{mp}, K_{sp}, C_2$ and C_3 from positive constants to positive-definite diagonal matrices. This needs a small change of $(1/(1 + C_2/C_3))(C_2/C_3)$ into $(\mathbf{I} + C_2C_3^{-1})^{-1}(C_2C_3^{-1})$ above and a similar small change in the transparency proof in the following, where $\mathbf{I}$ is the unit matrix.

4.3 Transparency Analysis

In this section, we use a unified Lyapunov function to show the transparency of the overall system based on the unified closed-loop obtained in Section 4.2.

Theorem 1: Assume the following conditions hold:

1) the Jacobian matrices $\mathbf{J}_m(\mathbf{q}_m)$ and $\mathbf{J}_s(\mathbf{q}_s)$ are nonsingular,

2) the inertia matrices $\widehat{\mathbf{M}}_{xm}(\mathbf{q}_m)$ and $\widehat{\mathbf{M}}_{xs}(\mathbf{q}_s)$ are invertible,

Consider the nonlinear teleoperation system (18)-(19) has uncertainties and is controlled by the adaptive controller (24)-(25) using the adaptation laws (26)-(27). Then, the signals $\Delta\mathbf{x}_m, \Delta\dot{\mathbf{x}}_m, \Delta\boldsymbol{\theta}_{md}$ and $\Delta\boldsymbol{\theta}_{sd}$ in the closed-loop system are bounded. Beside, the position tracking error $\Delta\mathbf{x}_m = \mathbf{x}_m - \mathbf{x}_s$ converges to zero as $t \rightarrow \infty$. Moreover, the force tracking error $\Delta\mathbf{f} = \mathbf{f}_m - \mathbf{f}_s$ also converges to zero as $t \rightarrow \infty$. ∎

Proof: Consider a unified Lyapunov function candidate as

$$V = \tfrac{1}{2}(\Delta\dot{\mathbf{x}}_m + \alpha\Delta\mathbf{x}_m)^T(\Delta\dot{\mathbf{x}}_m + \alpha\Delta\mathbf{x}_m) + \tfrac{1}{2}\Delta\mathbf{x}_m^T(K_p + \alpha K_v - \alpha^2)\Delta\mathbf{x}_m + \tfrac{1}{2}\Delta\boldsymbol{\theta}_{md}^T\mathbf{L}_{md}^{-1}\Delta\boldsymbol{\theta}_{md} + \tfrac{1}{2}\Delta\boldsymbol{\theta}_{sd}^T\mathbf{L}_{sd}^{-1}\Delta\boldsymbol{\theta}_{sd} \tag{40}$$

where α is a positive constant and is chosen such that $\alpha < K_v$ as mentioned in Section 4.2. The derivative of V along the trajectory of the unified closed-loop system (39) is

$$\dot{V} = (\Delta\dot{\mathbf{x}}_m + \alpha\Delta\mathbf{x}_m)^T(-K_v\Delta\dot{\mathbf{x}}_m - K_p\Delta\mathbf{x}_m + \boldsymbol{\Phi}_m\Delta\boldsymbol{\theta}_{md} - \boldsymbol{\Phi}_s\Delta\boldsymbol{\theta}_{sd} + \alpha\Delta\dot{\mathbf{x}}_m) + \Delta\dot{\mathbf{x}}_m^T(K_p + \alpha K_v - \alpha^2)\Delta\mathbf{x}_m$$

$$+\Delta\boldsymbol{\theta}_{md}^T\mathbf{L}_{md}^{-1}\dot{\widehat{\boldsymbol{\theta}}}_{md} + \Delta\boldsymbol{\theta}_{sd}^T\mathbf{L}_{sd}^{-1}\dot{\widehat{\boldsymbol{\theta}}}_{sd} \tag{41}$$

Because

$$-K_v\Delta\dot{\mathbf{x}}_m - K_p\Delta\mathbf{x}_m + \boldsymbol{\Phi}_m\Delta\boldsymbol{\theta}_{md} - \boldsymbol{\Phi}_s\Delta\boldsymbol{\theta}_{sd} + \alpha\Delta\dot{\mathbf{x}}_m = -(K_v - \alpha)\Delta\dot{\mathbf{x}}_m - K_p\Delta\mathbf{x}_m + \boldsymbol{\Phi}_m\Delta\boldsymbol{\theta}_{md} - \boldsymbol{\Phi}_s\Delta\boldsymbol{\theta}_{sd},$$

we get

$$\dot{V} = (\Delta\dot{\mathbf{x}}_m + \alpha\Delta\mathbf{x}_m)^T(-(K_v - \alpha)\Delta\dot{\mathbf{x}}_m - K_p\Delta\mathbf{x}_m + \boldsymbol{\Phi}_m\Delta\boldsymbol{\theta}_{md} - \boldsymbol{\Phi}_s\Delta\boldsymbol{\theta}_{sd}) + \Delta\dot{\mathbf{x}}_m^T(K_p + \alpha K_v - \alpha^2)\Delta\mathbf{x}_m$$

11

$$+\Delta\boldsymbol{\theta}_{md}^T\mathbf{L}_{md}^{-1}\dot{\widehat{\boldsymbol{\theta}}}_{md} + \Delta\boldsymbol{\theta}_{sd}^T\mathbf{L}_{sd}^{-1}\dot{\widehat{\boldsymbol{\theta}}}_{sd} \qquad (42)$$

Also, because

$$(\Delta\dot{\mathbf{x}}_m + \alpha\Delta\mathbf{x}_m)^T(-(K_v - \alpha)\Delta\dot{\mathbf{x}}_m - K_p\Delta\mathbf{x}_m) = -\Delta\dot{\mathbf{x}}_m^T(K_v - \alpha)\,\Delta\dot{\mathbf{x}}_m - \alpha\Delta\mathbf{x}_m^TK_p\Delta\mathbf{x}_m - \Delta\dot{\mathbf{x}}_m^T(K_p + \alpha K_v - \alpha^2)\Delta\mathbf{x}_m\,,$$

we have

$$\dot{V} = -\Delta\dot{\mathbf{x}}_m^T(K_v - \alpha)\,\Delta\dot{\mathbf{x}}_m - \alpha\Delta\mathbf{x}_m^TK_p\Delta\mathbf{x}_m - \Delta\dot{\mathbf{x}}_m^T(K_p + \alpha K_v - \alpha^2)\Delta\mathbf{x}_m + \Delta\dot{\mathbf{x}}_m^T(K_p + \alpha K_v - \alpha^2)\Delta\mathbf{x}_m$$

$$+(\Delta\dot{\mathbf{x}}_m + \alpha\Delta\mathbf{x}_m)^T\boldsymbol{\Phi}_m\Delta\boldsymbol{\theta}_{md} - (\Delta\dot{\mathbf{x}}_m + \alpha\Delta\mathbf{x}_m)^T\boldsymbol{\Phi}_s\Delta\boldsymbol{\theta}_{sd} + \Delta\boldsymbol{\theta}_{md}^T\mathbf{L}_{md}^{-1}\dot{\widehat{\boldsymbol{\theta}}}_{md} + \Delta\boldsymbol{\theta}_{sd}^T\mathbf{L}_{sd}^{-1}\dot{\widehat{\boldsymbol{\theta}}}_{sd}$$

$$= -\Delta\dot{\mathbf{x}}_m^T(K_v - \alpha)\,\Delta\dot{\mathbf{x}}_m - \alpha\Delta\mathbf{x}_m^TK_p\Delta\mathbf{x}_m + (\Delta\dot{\mathbf{x}}_m + \alpha\Delta\mathbf{x}_m)^T\boldsymbol{\Phi}_m\Delta\boldsymbol{\theta}_{md} - (\Delta\dot{\mathbf{x}}_m + \alpha\Delta\mathbf{x}_m)^T\boldsymbol{\Phi}_s\Delta\boldsymbol{\theta}_{sd}$$

$$+\Delta\boldsymbol{\theta}_{md}^T\mathbf{L}_{md}^{-1}\dot{\widehat{\boldsymbol{\theta}}}_{md} + \Delta\boldsymbol{\theta}_{sd}^T\mathbf{L}_{sd}^{-1}\dot{\widehat{\boldsymbol{\theta}}}_{sd} \qquad (43)$$

Substituting the adaptation laws (26)-(27) into (43), we get

$$\dot{V} = -\Delta\dot{\mathbf{x}}_m^T(K_v - \alpha)\,\Delta\dot{\mathbf{x}}_m - \alpha\Delta\mathbf{x}_m^TK_p\Delta\mathbf{x}_m - \Delta\boldsymbol{\theta}_{md}^T\mathbf{W}_m^T(\mathbf{W}_m\widehat{\boldsymbol{\theta}}_{md} - \mathbf{f}_{mw} - \mathbf{f}_{hw}) - \Delta\boldsymbol{\theta}_{sd}^T\mathbf{W}_s^T(\mathbf{W}_s\widehat{\boldsymbol{\theta}}_{sd} - \mathbf{f}_{sw} + \mathbf{f}_{ew}) \qquad (44)$$

Substituting the definitions of $\mathbf{f}_{mw}, \mathbf{f}_{hw}, \mathbf{f}_{sw}$ and $\mathbf{f}_{ew}$ into the (44), we have

$$\dot{V} = -\Delta\dot{\mathbf{x}}_m^T(K_v - \alpha)\,\Delta\dot{\mathbf{x}}_m - \alpha\Delta\mathbf{x}_m^TK_p\Delta\mathbf{x}_m$$

$$-\Delta\boldsymbol{\theta}_{md}^T\mathbf{W}_m^T[\mathbf{W}_m\widehat{\boldsymbol{\theta}}_{md} - \tfrac{\lambda}{s+\lambda}(\mathbf{f}_m + \mathbf{f}_h)] - \Delta\boldsymbol{\theta}_{sd}^T\mathbf{W}_s^T[\mathbf{W}_s\widehat{\boldsymbol{\theta}}_{sd} - \tfrac{\lambda}{s+\lambda}(\mathbf{f}_s - \mathbf{f}_e)] \qquad (45)$$

According to Property 1, we obtain

$$\dot{V} = -\Delta\dot{\mathbf{x}}_m^T(K_v - \alpha)\,\Delta\dot{\mathbf{x}}_m - \alpha\Delta\mathbf{x}_m^TK_p\Delta\mathbf{x}_m$$

$$-\Delta\boldsymbol{\theta}_{md}^T\mathbf{W}_m^T(\mathbf{W}_m\widehat{\boldsymbol{\theta}}_{md} - \tfrac{\lambda}{s+\lambda}\mathbf{Y}_{md}\boldsymbol{\theta}_{md}) - \Delta\boldsymbol{\theta}_{sd}^T\mathbf{W}_s^T(\mathbf{W}_s\widehat{\boldsymbol{\theta}}_{sd} - \tfrac{\lambda}{s+\lambda}\mathbf{Y}_{sd}\boldsymbol{\theta}_{sd}) \qquad (46)$$

According to the definitions of $\mathbf{W}_m$ and $\mathbf{W}_s$, (46) can be rewritten as

$$\dot{V} = -\Delta\dot{\mathbf{x}}_m^T(K_v - \alpha)\,\Delta\dot{\mathbf{x}}_m - \alpha\Delta\mathbf{x}_m^TK_p\Delta\mathbf{x}_m - \Delta\boldsymbol{\theta}_{md}^T\mathbf{W}_m^T(\mathbf{W}_m\widehat{\boldsymbol{\theta}}_{md} - \mathbf{W}_m\boldsymbol{\theta}_{md}) - \Delta\boldsymbol{\theta}_{sd}^T\mathbf{W}_s^T(\mathbf{W}_s\widehat{\boldsymbol{\theta}}_{sd} - \mathbf{W}_s\boldsymbol{\theta}_{sd})$$

$$= -\Delta\dot{\mathbf{x}}_m^T(K_v - \alpha)\,\Delta\dot{\mathbf{x}}_m - \alpha\Delta\mathbf{x}_m^TK_p\Delta\mathbf{x}_m - \Delta\boldsymbol{\theta}_{md}^T\mathbf{W}_m^T\mathbf{W}_m\Delta\boldsymbol{\theta}_{md} - \Delta\boldsymbol{\theta}_{sd}^T\mathbf{W}_s^T\mathbf{W}_s\Delta\boldsymbol{\theta}_{sd} \qquad (47)$$

From (40) we know that V is a function of $\Delta\dot{\mathbf{x}}_m, \Delta\mathbf{x}_m, \Delta\boldsymbol{\theta}_{md}$ and $\Delta\boldsymbol{\theta}_{sd}$, and V = 0 only when $\Delta\mathbf{x}_m = 0, \Delta\dot{\mathbf{x}}_m = 0, \Delta\boldsymbol{\theta}_{md} = 0$, and $\Delta\boldsymbol{\theta}_{sd} = 0$. On the other hand, when one or more of $\Delta\mathbf{x}_m, \Delta\dot{\mathbf{x}}_m, \Delta\boldsymbol{\theta}_{md}, \Delta\boldsymbol{\theta}_{sd}$ is nonzero, we have $V > 0$, as $K_p + \alpha K_v - \alpha^2$ is a positive constant, and $\mathbf{L}_{md}^{-1}, \mathbf{L}_{sd}^{-1}$ are symmetric positive-definite matrices. Therefore, V is a positive-definite function.

Furthermore, from (47) we know that $\dot{V}$ is also a function of $\Delta\dot{\mathbf{x}}_m, \Delta\mathbf{x}_m, \Delta\boldsymbol{\theta}_{md}$ and $\Delta\boldsymbol{\theta}_{sd}$, and $\dot{V} = 0$ can happen only when $\Delta\mathbf{x}_m = 0, \Delta\dot{\mathbf{x}}_m = 0, \Delta\boldsymbol{\theta}_{md} = 0$, and $\Delta\boldsymbol{\theta}_{sd} = 0$. On the other hand, when one or more of $\Delta\mathbf{x}_m, \Delta\dot{\mathbf{x}}_m, \Delta\boldsymbol{\theta}_{md}, \Delta\boldsymbol{\theta}_{sd}$ is nonzero, we have $\dot{V} < 0$. Therefore, $\dot{V}$ a is negative-definite function.

Since V is positive definite and $\dot{V}$ is negative definite, V is bounded, the signals $\Delta\mathbf{x}_m, \Delta\dot{\mathbf{x}}_m, \Delta\boldsymbol{\theta}_{md}$ and $\Delta\boldsymbol{\theta}_{sd}$ in the closed-loop system are bounded, and also $\Delta\mathbf{x}_m, \Delta\dot{\mathbf{x}}_m, \Delta\boldsymbol{\theta}_{md}$ and $\Delta\boldsymbol{\theta}_{sd}$ approach zero as $t \to \infty$. In other words, in terms of position tracking, we have $\lim_{t\to\infty}\Delta\mathbf{x}_m = \lim_{t\to\infty}(\mathbf{x}_m - \mathbf{x}_s) = 0$.

In terms of force tracking convergence, we note that $\Delta\mathbf{x}_m, \Delta\dot{\mathbf{x}}_m, \Delta\boldsymbol{\theta}_{md}$ and $\Delta\boldsymbol{\theta}_{sd}$ approach zero as $t \to \infty$. Thus, according to the unified closed-loop (39), we can get $\lim_{t\to\infty}\Delta\ddot{\mathbf{x}}_m = 0$. Furthermore, according to the master and the slave closed-loop (36)-(37), the force tracking error $\Delta\mathbf{f} = \mathbf{f}_h - \mathbf{f}_e \to 0$ as $t \to \infty$. This concludes the proof.

Remark 3: The estimated inertia matrices $\widehat{\mathbf{M}}_{xm}(\mathbf{q}_m)$ and $\widehat{\mathbf{M}}_{xs}(\mathbf{q}_s)$ for the master and the slave are assumed to be invertible. To remove this assumption, in the controllers (24)-(27), $\widehat{\mathbf{M}}_{xm}(\mathbf{q}_m)$ and $\widehat{\mathbf{M}}_{xs}(\mathbf{q}_s)$ can be replaced by their

priori estimates $\widehat{\mathbf{Mp}}_{xm}$ and $\widehat{\mathbf{Mp}}_{xs}$, respectively, where $\widehat{\mathbf{Mp}}_{xm} = \widehat{\mathbf{Mp}}_{xm}^{\mathbf{T}} \geq \mathbf{0}$ and $\widehat{\mathbf{Mp}}_{xs} = \widehat{\mathbf{Mp}}_{xs}^{\mathbf{T}} \geq \mathbf{0}$. Since $\widehat{\mathbf{Mp}}_{xm}$ and $\widehat{\mathbf{Mp}}_{xs}$ are not updated online, the invertibility of $\widehat{\mathbf{Mp}}_{xm}$ and $\widehat{\mathbf{Mp}}_{xs}$ is not a concern. More details about this can be found in [18], [20].

5. CONTROLLERS FOR UNCERTAIN MODELS OF OPERATOR AND ENVIRONMENT

In the adaptive control laws (24)-(25) in Section 4, the interaction force between the master and the operator $\mathbf{f}_h$, and the interaction force between the slave and the environment $\mathbf{f}_e$ can be measured by force sensors and thus are directly included in order to cancel the same terms in the master and the slave dynamics (18)-(19). Alternatively, $\mathbf{f}_h$ and $\mathbf{f}_e$ in (18)-(19) can be replaced by dynamic models of the operator and the environment respectively, i.e., by the following general forms [14], [15], [16], [27]

$$\mathbf{f}_h = \mathbf{f}_h^* - (\mathbf{M}_h \ddot{\mathbf{x}}_m + \mathbf{B}_h \dot{\mathbf{x}}_m + \mathbf{K}_h \mathbf{x}_m) \tag{48}$$

$$\mathbf{f}_e = \mathbf{M}_e \ddot{\mathbf{x}}_s + \mathbf{B}_e \dot{\mathbf{x}}_s + \mathbf{K}_e \mathbf{x}_s \tag{49}$$

where $\mathbf{M}_h, \mathbf{M}_e, \mathbf{B}_h, \mathbf{B}_e, \mathbf{K}_h$ and $\mathbf{K}_e$ are matrices in $R^{6\times6}$ corresponding to the mass, damping, and stiffness of the operator's hand and the environment, respectively. Also, $\mathbf{h}(.) \in R^n \to R^6$ is a nonlinear transformation describing the relation between the joint-space and the Cartesian-space position (and orientation) of each robot, i.e., $\mathbf{x}_m = \mathbf{h}_m(\mathbf{q}_m)$ and $\mathbf{x}_s = \mathbf{h}_s(\mathbf{q}_s)$.

Substituting (48)-(49) into (18)-(19), a combined model for master/operator and another combined model for slave/environment are obtained as

$$\mathbf{M}_{mo}(\mathbf{q}_m)\ddot{\mathbf{x}}_m + \mathbf{C}_{mo}(\mathbf{q}_m, \dot{\mathbf{q}}_m)\dot{\mathbf{x}}_m + \mathbf{G}_{mo}(\mathbf{q}_m) = \mathbf{f}_m \tag{50}$$

$$\mathbf{M}_{se}(\mathbf{q}_s)\ddot{\mathbf{x}}_s + \mathbf{C}_{se}(\mathbf{q}_s, \dot{\mathbf{q}}_s)\dot{\mathbf{x}}_s + \mathbf{G}_{se}(\mathbf{q}_s) = \mathbf{f}_s \tag{51}$$

where

$$\mathbf{M}_{mo}(\mathbf{q}_m) = \mathbf{M}_{xm}(\mathbf{q}_m) + \mathbf{M}_h, \mathbf{C}_{mo}(\mathbf{q}_m, \dot{\mathbf{q}}_m) = \mathbf{C}_{xm}(\mathbf{q}_m, \dot{\mathbf{q}}_m) + \mathbf{B}_h, \mathbf{G}_{mo}(\mathbf{q}_m) = \mathbf{G}_{xm}(\mathbf{q}_m) + \mathbf{K}_h \mathbf{h}_m(\mathbf{q}_m) - \mathbf{f}_h^*$$

$$\mathbf{M}_{se}(\mathbf{q}_s) = \mathbf{M}_{xs}(\mathbf{q}_s) + \mathbf{M}_e, \mathbf{C}_{se}(\mathbf{q}_s, \dot{\mathbf{q}}_s) = \mathbf{C}_{xs}(\mathbf{q}_s, \dot{\mathbf{q}}_s) + \mathbf{B}_e, \mathbf{G}_{se}(\mathbf{q}_s) = \mathbf{G}_{xs}(\mathbf{q}_s) + \mathbf{K}_e \mathbf{h}_s(\mathbf{q}_s)$$

For the combined models (50) and (51), the adaptive inverse dynamics 4-channel control scheme can be designed as follows:

- Control laws for the master and the slave:

$$\mathbf{f}_m = \widehat{\mathbf{M}}_{mo}(\mathbf{q}_m)(\ddot{\mathbf{x}}_s - \mathbf{K}_{mv}\Delta\dot{\mathbf{x}}_m - \mathbf{K}_{mp}\Delta\mathbf{x}_m) + \widehat{\mathbf{C}}_{mo}(\mathbf{q}_m, \dot{\mathbf{q}}_m)\dot{\mathbf{x}}_m + \widehat{\mathbf{G}}_{mo}(\mathbf{q}_m) + \widehat{\mathbf{M}}_{mo}(\mathbf{q}_m)C_2(\mathbf{f}_h - \mathbf{f}_e) \tag{52}$$

$$\mathbf{f}_s = \widehat{\mathbf{M}}_{se}(\mathbf{q}_s)(\ddot{\mathbf{x}}_m - \mathbf{K}_{sv}\Delta\dot{\mathbf{x}}_s - \mathbf{K}_{sp}\Delta\mathbf{x}_s) + \widehat{\mathbf{C}}_{se}(\mathbf{q}_s, \dot{\mathbf{q}}_s)\dot{\mathbf{x}}_s + \widehat{\mathbf{G}}_{se}(\mathbf{q}_s) + \widehat{\mathbf{M}}_{se}(\mathbf{q}_s)C_3(\mathbf{f}_h - \mathbf{f}_e) \tag{53}$$

- Adaptation laws:

$$\dot{\hat{\boldsymbol{\theta}}}_{mod} = -\mathbf{L}_{mod}[\boldsymbol{\Phi}_{mo}^{\mathbf{T}}(\Delta\dot{\mathbf{x}}_m + \alpha\Delta\mathbf{x}_m) + \mathbf{W}_{mo}^{\mathbf{T}}\mathbf{E}_{mo}] \tag{54}$$

$$\dot{\hat{\boldsymbol{\theta}}}_{sed} = -\mathbf{L}_{sed}[\boldsymbol{\Phi}_{se}^{\mathbf{T}}(\Delta\dot{\mathbf{x}}_s + \alpha\Delta\mathbf{x}_s) + \mathbf{W}_{se}^{\mathbf{T}}\mathbf{E}_{se}] \tag{55}$$

where $\mathbf{L}_{mod}$ and $\mathbf{L}_{sed}$ are symmetric positive-definite matrices and $\boldsymbol{\theta}_{mod}$ includes the dynamic parameters of the master and the human, $\boldsymbol{\theta}_{sed}$ includes the dynamic parameters of the slave and the environment. Also,

$$\boldsymbol{\Phi}_{mo} = (1/(1 + C_2/C_3))\widehat{\mathbf{M}}_{mo}^{-1}(\mathbf{q}_m)\mathbf{Y}_{mod} \tag{56}$$

$$\boldsymbol{\Phi}_{se} = (1/(1 + C_2/C_3))(C_2/C_3)\widehat{\mathbf{M}}_{se}^{-1}(\mathbf{q}_s)\mathbf{Y}_{sed} \tag{57}$$

where $\mathbf{Y}_{mod}$ and $\mathbf{Y}_{sed}$ are the corresponding dynamic regressor matrices. Besides, $\mathbf{W}_{mo}$ and $\mathbf{W}_{se}$ are the filtered versions of the dynamic regressor matrices $\mathbf{Y}_{mod}$ and $\mathbf{Y}_{sed}$, $\mathbf{E}_{mo}$ and $\mathbf{E}_{se}$ are the filtered prediction errors of the filtered inputs $\mathbf{f}_{mw}$ ($\mathbf{f}_{mw}$ is the filtered version of $\mathbf{f}_m$) and $\mathbf{f}_{sw}$ ($\mathbf{f}_{sw}$ is the filtered version of $\mathbf{f}_s$). The proof of position/force error convergence for this case is similar to that of Theorem 1.

Remark 4: It should be noted that $\mathbf{f}_h$ in (24) and $\mathbf{f}_e$ in (25) do not exist in (52) and (53) as they have been incorporated into the dynamics of the master and the slave, respectively.

6. SIMULATION STUDIES

In this section, simulations are conducted to illustrate the performance of the proposed controllers (24)-(27). Consider identical master and slave robots to be the 2-DOF planar manipulator in Fig. 5, which consists of two links and two rotary joints. The inertia matrix, Coriolis and centrifugal vector, gravity term, and Jacobian matrix of the robot are as follows:

$$\mathbf{M}(\mathbf{q}) = \begin{bmatrix} l_2^2 m_2 + 2l_1 l_2 m_2 \cos(q_2) + l_1^2(m_1 + m_2) & l_2^2 m_2 + l_1 l_2 m_2 \cos(q_2) \\ l_2^2 m_2 + l_1 l_2 m_2 \cos(q_2) & l_2^2 m_2 \end{bmatrix},$$

$$\mathbf{C}(\mathbf{q}, \dot{\mathbf{q}}) = \begin{bmatrix} -2l_1 l_2 m_2 \sin(q_2) \dot{q}_2 & -l_1 l_2 m_2 \sin(q_2) \dot{q}_2 \\ l_1 l_2 m_2 \sin(q_2) \dot{q}_2 & 0 \end{bmatrix},$$

$$\mathbf{G}(\mathbf{q}) = \begin{bmatrix} m_2 l_2 g \cos(q_1 + q_2) + (m_1 + m_2) l_1 g \cos(q_1) \\ m_2 l_2 g \cos(q_1 + q_2) \end{bmatrix},$$

$$\mathbf{J}(\mathbf{q}) = \begin{bmatrix} l_1 \sin(q_2) & 0 \\ l_1 \cos(q_2) + l_2 & l_2 \end{bmatrix},$$

where l_1 and l_2 are the lengths of the links, m_1 and m_2 are the point masses of the links, g is the gravity constant, and $\mathbf{q} = [q_1, \ q_2]^T$. After transforming the dynamics from the joint space to the Cartesian space according to (10)-(17), the dynamics parameters vector can be found as $\boldsymbol{\theta} = [m_2, \ m_1, \ m_2 l_2 / l_1]^T$. Then, according to Property 1, the regressor matrix $\mathbf{Y}(\mathbf{q}, \dot{\mathbf{q}}, \dot{\mathbf{x}}, \ddot{\mathbf{x}})$ can be obtained.
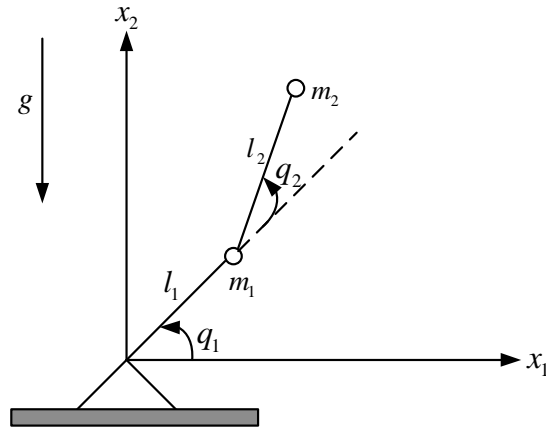

Fig. 5 2-DOF planar manipulator

As for the operator and the environment models, we employ (48)-(49), and take

$$\mathbf{M}_h = m_h \mathbf{I}, \mathbf{B}_h = b_h \mathbf{I}, \ \mathbf{K}_h = k_h \mathbf{I}, \ \mathbf{M}_e = m_e \mathbf{I}, \mathbf{B}_e = b_e \mathbf{I}, \ \mathbf{K}_e = k_e \mathbf{I},$$

where m_h, m_e, b_h, b_e, k_h and k_e are the mass, damping, and stiffness coefficients of the operator's hand and the environment, respectively. As in practice, the input $\mathbf{f}_h^*$ starts from a zero value in $\mathbf{f}_h^* = [50\sin(2.5t), 0]^T$.

In the simulation, the parameters of the master and slave (chosen from [25]), the operator and the environment (chosen from [27]), and the controllers, are given in Table 2. According to Table 2, the actual parameter vectors are $\boldsymbol{\theta}_{md} = \boldsymbol{\theta}_{sd} = [4.6, 2.3, 4.6]^T$. In the simulations, the initial positions of the master and the slave are set to be $\mathbf{x}_m(0) = \mathbf{x}_s(0) = [-0.05, 0.3794]^T$, and the initial estimates of uncertain parameter vectors are assumed to be $\widehat{\boldsymbol{\theta}}_{md}(0) = \widehat{\boldsymbol{\theta}}_{sd}(0) = [3.68, 1.84, 3.68]^T$.

Table 2: Model parameters used in the simulation

| m_1	m_2	l_1	l_2	g	m_h
2.3kg	4.6kg	0.5m	0.5m	9.8kg.m/s^2	3.25kg
b_h	k_h	m_e	b_e	ke	K_{mv}, K_{sv}
20 Nsm^{-1}	300 Nm^{-1}	1kg	40 Nsm^{-1}	1500 Nm^{-1}	1
K_{mp}, K_{sp}	α	λ	C_2, C_3	$\mathbf{L}_{md}, \mathbf{L}_{sd}$	
2	0.1	800	0.05	0.1$\mathbf{I}$	

The simulation results in terms of master/slave position and force profiles in the x_1-direction are shown in Fig. 6(a)-(d). It can be seen that the slave can track the position and force of the master very well even though there are parametric uncertainties in the master and slave models. Note that due to the lack of excitation in the x_2-direction (because $\mathbf{f}_h^* = [50\sin(2.5t), 0]^T$)), perfect position and force tracking exist in that direction and, therefore, the results have not been shown.

It should be noted that, in the control laws (24)-(25), it is assumed that the accelerations $\ddot{\mathbf{x}}_m$ and $\ddot{\mathbf{x}}_s$ can be measured. Thus, in order to see how the designed controller will work under noises in acceleration measurement, we introduce noises in the position measurements and force measurements in the simulation. The corresponding results are shown in Fig. 7(a)-(d). The results show that the slave tracks the position of the master well even when there are measurement noises in the system, although a small force tracking error exists.

The performance of the proposed adaptive inverse dynamics control approach is also compared with the approach in [10], in which the standard Slotine&Li adaptive position controllers [17] is used inside a 4-channel bilateral teleoperation system. The results of the approach in [10] are shown in Fig. 8(a)-(d). Comparing Fig. 6 with Fig. 8, it can be found that the performance of the proposed adaptive controller is better.
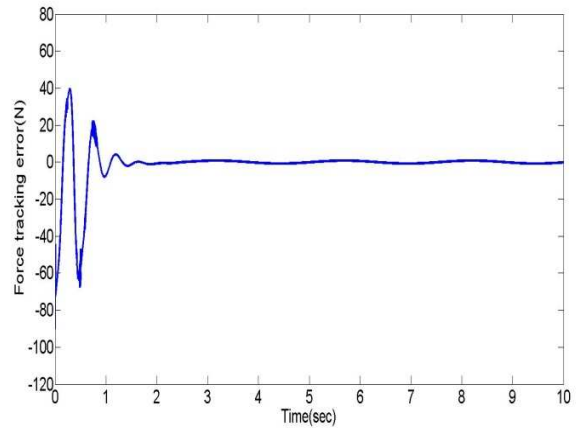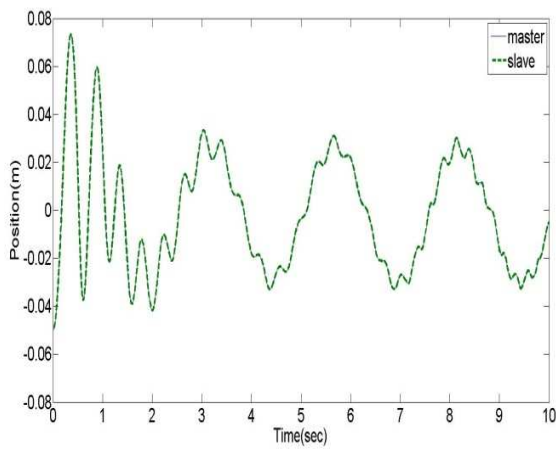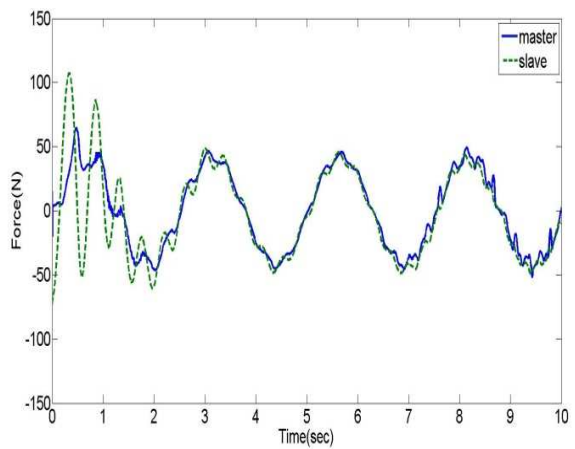
15
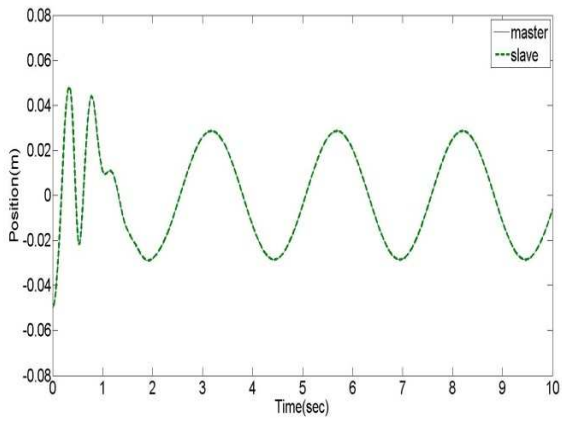
(a)
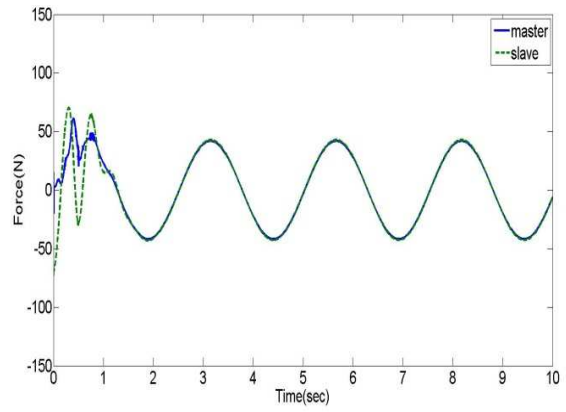
(c)
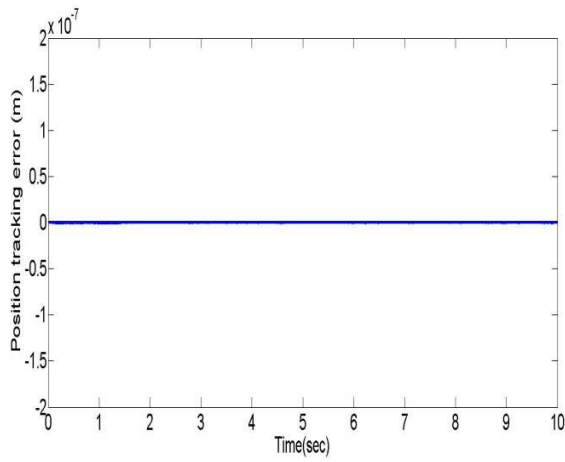
(b)

(d)

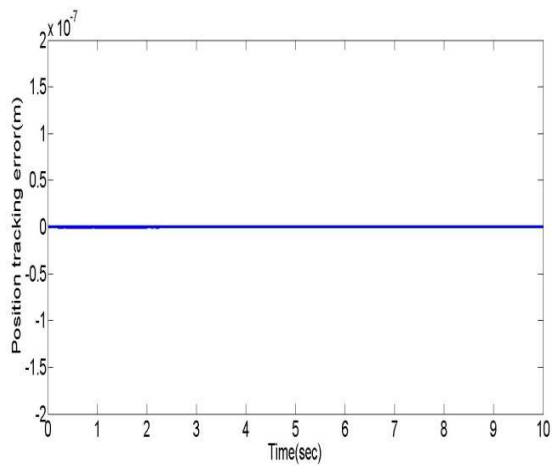Fig. 6 Proposed adaptive control

(a) Position tracking, (b) Position tracking error, (c) Force tracking, (d) Force tracking error

(a)

(c)
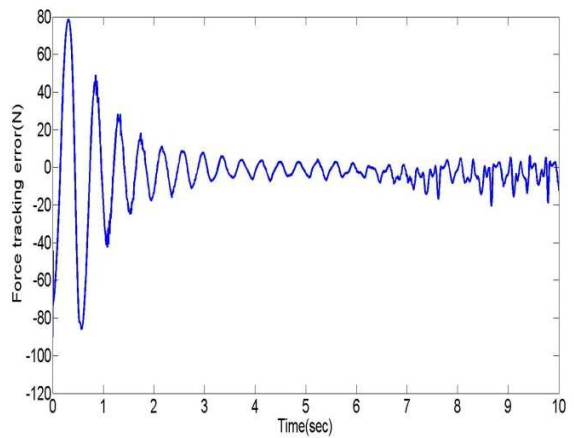
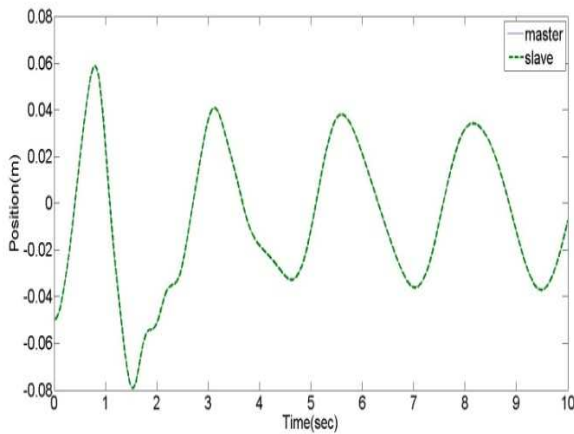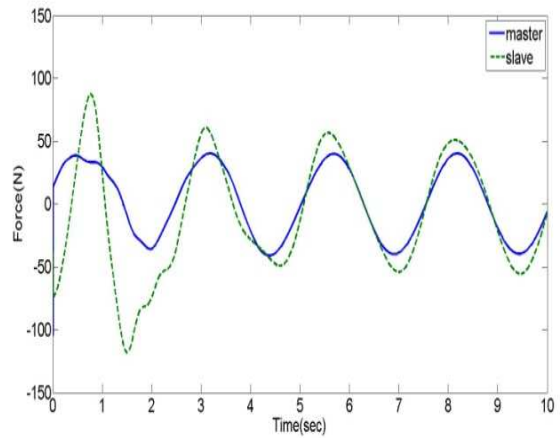(b)   (d)

Fig. 7 Proposed adaptive control in the presence of measurement noise

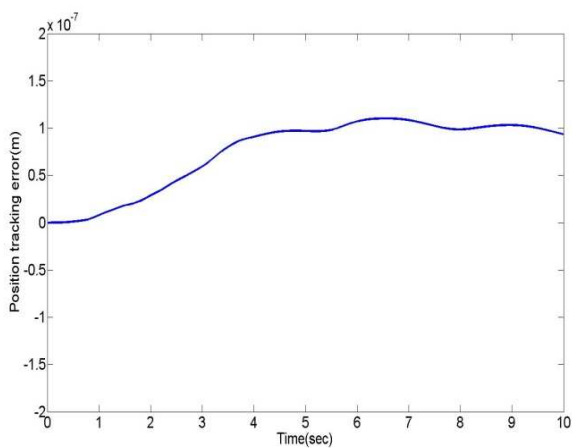(a) Position tracking, (b) Position tracking error, (c) Force tracking, (d) Force tracking error

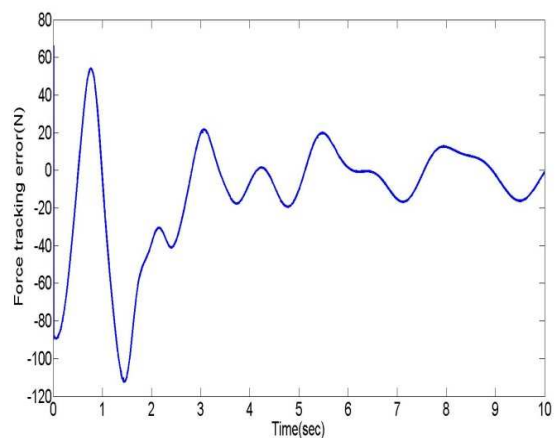(a)   (c)

(b)   (d)

Fig. 8 Standard Slotine & Li adaptive control (in the absence of measurement noise)

(a) Position tracking, (b) Position tracking error, (c) Force tracking, (d) Force tracking error

7. CONCLUSIONS

In this paper, an adaptive control method based on the inverse dynamics approach and the 4-channel bilateral teleoperation architecture is developed for uncertain and nonlinear haptic teleoperation systems. The adaptive controllers designed for the master and the slave robots do not need perfect knowledge of the dynamics of the master, the slave, the human operator, or the environment. A unified closed-loop dynamics is developed for the overall teleoperation system and a unified Lyapunov function is presented to prove the transparency. An alternative control scheme is also discussed, which incorporates the uncertain dynamic models of the operator and the environment into the master and the slave, respectively. Simulation studies are presented to show the effectiveness of the proposed approach. Compared with other adaptive control schemes for teleoperation systems, the proposed adaptive controller can yield linear error dynamics, which becomes decoupled when the uncertain parameters converge to their true values. Consequently, the transparency of the closed-loop system is more convenient to study.

A potential issue with control laws (24)-(25) is the assumption that the accelerations $\ddot{x}_m$ and $\ddot{x}_s$ are measured. The same assumption is regularly made for achieving full transparency in the original 4-channel teleoperation architecture. Indeed, the controllers C_1 and C_4 in the original 4-channel design require acceleration measurements to be able to guarantee asymptotic position tracking ($\ddot{e} + k_v \dot{e} + k_p e = 0$, where e is the position error) given the inertia contributions of the master and slave dynamics [6], [7]. It must be noted, however, that near-transparency can be obtained at low frequencies by ignoring these acceleration terms. Indeed, since voluntary motions of the human hand are themselves band-limited[1], in the absence of acceleration measurements, position and force tracking will be good short of feeling high-frequency phenomena such as the sharp edges or texture of an object. On the other hand, if perfect transparency over a large bandwidth is required, using accelerometers may be justifiable. Alternatively, it is possible to use position measurements with differentiators that are robust to measurement noise. For instance, Levant [30] designed a robust exact differentiator, and Suzuki et al [31] proposed an adaptive version of Levant's differentiator. Sidhom et al [32] dealt with the use of Suzuki's differentiator in an identification context. Incorporating such robust differentiators in our adaptive control scheme to eliminate the need for acceleration measurement remains as future work.

REFERENCES

[1] S. Salcudean, "Control for teleoperation and haptic interfaces," Control Problems in Robotics and Automation, Eds. New York: Springer-Verlag, pp. 51-56 (1998).

[2] C. Melchiorri, "Robotic telemanipulation systems: An overview on control aspects," in Proceeding of 7th IFAC Sympos. on Robot Control, Sept. , Wroclaw, Poland, pp. 707–716 (2003).

[3] P. Hokayem and M. Spong, "Bilateral teleoperation: an historical survey," Automatica, vol. 42, no. 12, pp. 2035-2057 (2006).

[4] J. E. Colgate, "Robust impedance shaping telemanipulation," IEEE Transactions on Robotics and Automation, vol. 9, no.4, pp.374-384 (1993).

---

[1] The maximum bandwidth with which the human finger can apply motion or force commands is 5-10 Hz [28] and the maximum bandwidth with which the human finger reacts to tactile stimuli is 8-10 Hz [29].

[5] L. Lee and P. Y. Li, "Passive bilateral feedforward control of linear dynamically similar teleoperated manipulators," IEEE Transactions on Robotics and Automation, vol. 19, no. 3, pp.443-456 (2003).

[6] D. A. Lawrence, "Stability and transparency in bilateral teleoperation," IEEE Transactions on Robotics and Automation, vol. 9, no. 5, pp. 624-637 (1993).

[7] Y. Yokokohji and T. Yoshikawa, "Bilateral control of master-slave manipulator for ideal kinesthetic coupling-formulation and experiment," IEEE Transactions on Robotics and Automation, vol. 10, no. 5, pp. 605-619 (1994).

[8] Hyoung-Ki Lee and M. J. Chung, "Adaptive controller of a master-slave system for transparent teleoperation," Journal of Robotic systems, vol. 15, no. 8, pp. 465-475 (1998).

[9] M. Shi, G. Tao and H. Liu, "Adaptive control of teleoperation systems," Journal of X-Ray Science and Technology, vol. 10, no. 1-2, pp. 37-57 (2002).

[10] J. H. Ryu and D. S. Kwon, "A novel adaptive bilateral control scheme using similar closed-loop dynamic characteristics of master/slave manipulators," Journal of Robotic Systems, vol. 18, no. 9, pp. 533-543 (2001).

[11] N. V. Q. Hung, T. Narikiyo and H. D. Tuan, "Nonlinear adaptive control of master-slave system in teleoperation," Control Engineering Practice, vol. 11, no. 1, pp. 1-10 (2003).

[12] N. Chopra, M. W. Spong and R. Lozano, "Synchronization of bilateral teleoperators with time delay," Automatica, vol. 44, no. 8, pp. 2142-2148 (2008).

[13] E. Nuño, R. Ortega and L. Basañez, "An adaptive controller for nonlinear teleoperators," Automatica, vol. 46, no. 1, pp. 155-159 (2010).

[14] Wen-Hong Zhu and S. E. Salcudean, "Stability guaranteed teleoperation: an adaptive motion/force control approach," IEEE transactions on automatic control, vol. 45, no. 11, pp. 1951-1969 (2000).

[15] S. Sirouspour and P. Setoodeh, "Adaptive nonlinear teleoperation control in multi-master/multi-slave environments," in Proceeding of the IEEE Conference on Control Applications, Toronto, Canada, August, pp. 1263-1268 (2005).

[16] P. Malysz and S. Sirouspour, "Nonlinear and filtered force/position mapping in bilateral teleoperation with application to enhanced stiffness discrimination," IEEE Transactions on Robotics, vol. 25, no. 5, pp. 1134-1149 (2009).

[17] J. J. E. Slotine and W. Li, Applied nonlinear control, Prentice-Hall, Englewood Cliffs, NJ (1991).

[18] M.W. Spong and R. Ortega, "On adaptive inverse dynamics control of rigid robots," IEEE Transactions on Automatic Control, vol. 35, no. 1, pp. 92-95 (1990).

[19] D. M. Dawson and F. L. Lewis, "Comments on 'on adaptive inverse dynamics control of rigid robots'," IEEE Transactions on Automatic Control, vol. 36, no. 10, pp. 1215-1216 (1991).

[20] H. Wang and Y. Xie, "Adaptive inverse dynamics control of robots with uncertain kinematics and dynamics", Automatica, vol. 45, no.9, pp. 2114-2119 (2009).

[21] K. Hashtrudi-Zaad, S. Salcudean, "Analysis of control architectures for teleoperation systems with impedance/admittance master and slave manipulators," The International Journal of Robotics Research, vol. 20, no.6, pp. 419-445 (2001).

[22] P. Arcara and C. Melchiorri, "Control schemes for teleoperation with time delay: A comparative study," Robotics and Autonomous Systems, vol. 38, no. 1, pp. 49-64 (2002).

[23] Aliaga, A. Rubio, and E. Sanchez, "Experimental quantitative comparison of different control architectures for master-slave teleoperation," IEEE Transactions on Control Systems Technology, vol.12, no.1, pp. 2-11 (2004).

[24] M. Tavakoli, A. Aziminejad, R.V. Patel and M. Moallem, "High-fidelity bilateral teleoperation systems and the effect of multimodal haptics," IEEE Transactions on Systems, Man, and Cybernetics - Part B, vol. 37, no.6, pp. 1512-1528 (2007).

[25] J. Craig, Introduction to robotics: mechanics and control (3rd Ed.), Pearson Prentice Hall, USA (2005).

[26] M. W. Spong, S. Hutchinson, M. Vidyasagar, Robot modeling and control, Wiley (2005).

[27] J. E. Speich, L. Shao and M. Goldfarb, "Modeling the human hand as it interacts with a telemanipulation system," Mechatronics, vol. 15, no. 9, pp. 1127-1142 (2005).

[28] K.B. Shimoga, "A survey of perceptual feedback issues in dexterous telemanipulation: Part I. Finger force feedback," Proceedings in IEEE Virtual Reality Annual International Symposium, pp. 263–270 (1993).

[29] K.B. Shimoga, "A survey of perceptual feedback issues in dexterous telemanipulation: Part II. Finger touch feedback," Proceedings in IEEE Virtual Reality Annual International Symposium, pp. 271–279 (1993).

[30] A. Levant, "Robust exact differentiation via sliding mode technique," Automatica, vol. 34, no. 3, pp. 379-384 (1998).

[31] S. Suzuki, K. Furuta, and S. Shiratori, "Adaptive impact shot control by pendulum-like juggling system," JSME International Journal, vol. 46, no. 3, pp. 973-981 (2003).

[32] L. Sidhom, M.T. Pham, F. Th´evenoux and M. Gautier, "Identification of a robot manipulator based on an adaptive higher order sliding modes differentiator," IEEE/ASME International Conference on Advanced Intelligent Mechatronics, Montréal, Canada, July (2010).